Carrier-induced noncollinear magnetism in perovskite manganites by first-principles calculations

メタデータ	言語: eng
	出版者:
	公開日: 2017-10-03
	キーワード (Ja):
	キーワード (En):
	作成者:
	メールアドレス:
	所属:
URL	https://doi.org/10.24517/00010973

Carrier-induced Noncollinear Magnetism in Perovskite Manganites by First-principles Calculation

K. Sawada[1] **and F. Ishii**[1,2]

[1]Division of Mathematical and Physical Science, Graduate School of Natural Science and Technology, Kanazawa University, Kakuma, Kanazawa 920-1192, Japan
[2]Reserach Institute for Computational Sciences, National Institute of Advanced Industrial Science and Technology (RICS-AIST), 1-1-1 Umezono, Tsukuba, Ibaraki 305-8568, Japan

E-mail: `sawada@cphys.s.kanazawa-u.ac.jp`

Abstract. We have performed noncollinear first-principles density functional calculations of carrier-doped perovskite manganites $La_{1-x}Sr_xMnO_3$ ($0.0 \leq x \leq 1.0$). In the calculated magnetic phase diagram ($T = 0$) within the collinear magnetic configurations, ferromagnetic and several antiferromagnetic configurations successively appeared as a ground state with increasing x. The calculated total energies of the ferromagnetic and A-type antiferromagnetic phases are almost degenerate around the phase boundary, $x = 0.5$. We found that the noncollinear magnetic configurations are stable in a wide range of carrier concentrations $0.3 \leq x \leq 0.6$. We discussed the effect of lattice distortions on the stability of the noncollinear magnetic phase.

1. Introduction

Perovskite manganites $La_{1-x}Sr_xMnO_3$ (LSMO) exhibit novel physical properties such as colossal magnetoresistance[1] and half-metallicity[2]. These novel physical properties originate from a variety of magnetic configurations in LSMO such as ferromagnetic (FM), A-type (interplane antiferromagnetic (AFM) and intraplane FM orders), C-type (interplane FM and intraplane AFM orders) and G-type (interplane AFM and intraplane AFM orders) AFM states (See Fig. 1 (a)). These magnetic states are controlled by the carrier concentrations and lattice distortions in LSMO[3, 4]. An experimental study revealed that the magnetic phase changes as AFM-A $\rightarrow$ FM $\rightarrow$ AFM-A $\rightarrow$ AFM-C $\rightarrow$ AFM-G states with increasing carrier concentrations in LSMO[5].

The magnetic states around the phase boundary in carrier-doped manganite have been extensively discussed on the basis of the long-range ordered *noncollinear* spin-canting magnetic (SCM) states or the coexistence of AFM and FM states, i.e., phase separation. While the SCM state was suggested as a possible ground state with competition between magnetic interactions[6, 7, 8], the FM–AFM phase separation was also suggested as a stable phase by an experimental study and model calculations[9, 10, 11]. Despite the extensive studies on the magnetic state around the phase boundary, the issue remains unresolved. Similar problems are encountered in the interface of artificial superlattices[12, 13, 14] such as $(LaMnO_3)_m/(SrMnO_3)_n$ where inhomogeneous carriers are introduced. In order to design magnetic states in the artificial superlattice, a detailed systematic study of the carrier-dependence of magnetism in LSMO is of great importance.

In this study, we have performed noncollinear first-principles density-functional calculations on the carrier-doped perovskite manganites LSMO and clarified the possibility of carrier-induced noncollinear magnetism. The noncollinear magnetic states are stable around the region of half-doping carrier concentrations. We discussed the effect of lattice distortion on the stability of noncollinear magnetism.

2. Computational Methods

We have performed first-principles calculations on $La_{1-x}Sr_xMnO_3$ ($0.0 \leq x \leq 1.0$) by the noncollinear density functional theory (DFT)[15, 16]. A generalized gradient approximation (GGA)[17] is adopted to determine the exchange correlation potential after the diagonalization of the noncollinear spin-density matrix. The norm-conserving pseudopotential method[18] with a partial core correction[19] is used and wavefunctions are expanded by a linear combination of multiple pseudo-atomic orbitals (LCPAO) [20, 21]. Three valence orbitals (*s*-, *p*- and *d*-orbitals) along with the polarization orbital (*f*-orbital) for La atoms, three valence orbitals (*s*-, *p*- and *d*-orbitals) without the polarization orbital (*f*-orbital) for Mn atoms and two valence orbitals (*s*- and *p*-orbitals) without the polarization orbital (*d*-orbital) for O atoms are used as a basis set. The *k*-point sampling of a uniform mesh 6 $\times$ 6 $\times$ 4 is used. The total energy difference
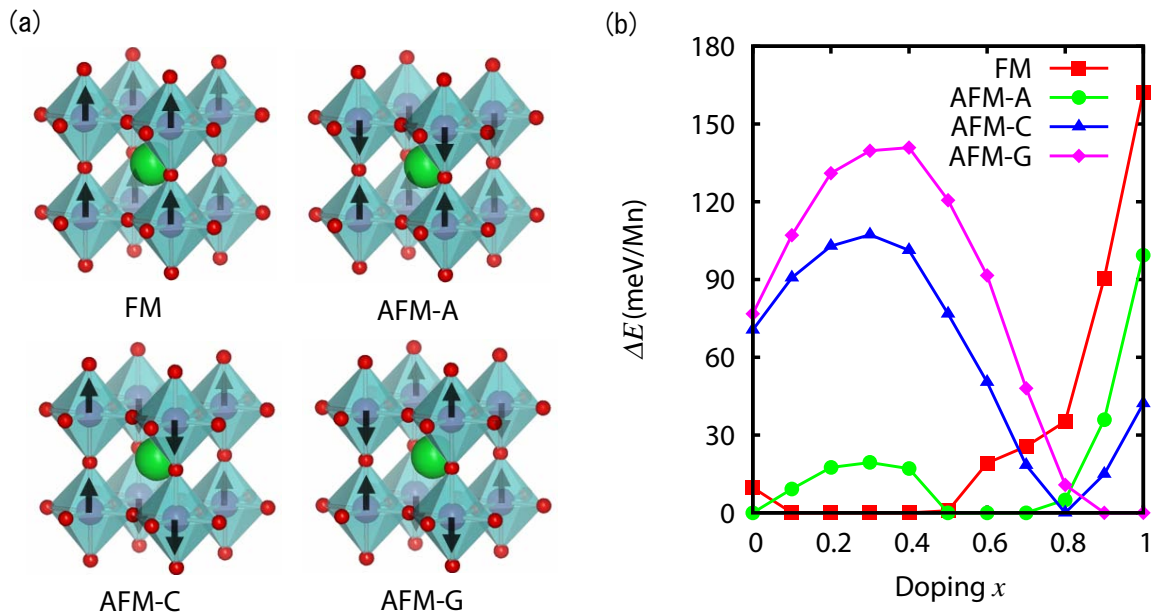
Figure 1. (a) The collinear magnetic structures of La$_{1-x}$Sr$_x$MnO$_3$. (b) The total energy difference per Mn atom from the stable state as a function of x. The red squares, green circles, blue triangles and pink diamonds denote the FM, AFM-A, AFM-C and AFM-G states, respectively. The lines serve as a visual reference.

between the FM and the AFM-A states converged within 2.2 meV/Mn for the k-point sampling. We neglected the spin-orbit interactions in all calculations. The calculations were done for a four-formula unit cell, i.e., 20 atoms in the unit cell. Hole carrier doping x is performed by a shift in the Fermi level and a uniform background charge is introduced to balance the charge neutrality of the system. Noncollinear spin orientations are fixed by using constrained DFT, where the penalty functions are introduced in the total-energy functional[22, 23]. All the above methods are implemented in OPENMX code[24]. In order to check the reliability of the pseudopotentials and convergence of LCPAOs, we confirmed that our calculated magnetic ground state in LaMnO$_3$ is consistent with previous results calculated by the all-electron full-potential linear augmented plane wave (FLAPW) method[25]. The pseudopotential method with LCPAO has also been successfully applied to Mn clusters[26, 27] and bulk transition metal oxides[28, 29]. We use the atomic coordinates of orthorhombic LaMnO$_3$ ($x = 0.0$) and the cubic SrMnO$_3$ ($x = 1.0$) determined by experimental studies[30, 31]. In the region of $0.0 < x < 1.0$, we assumed that the lattice structure is continuously changed from LaMnO$_3$ to SrMnO$_3$.
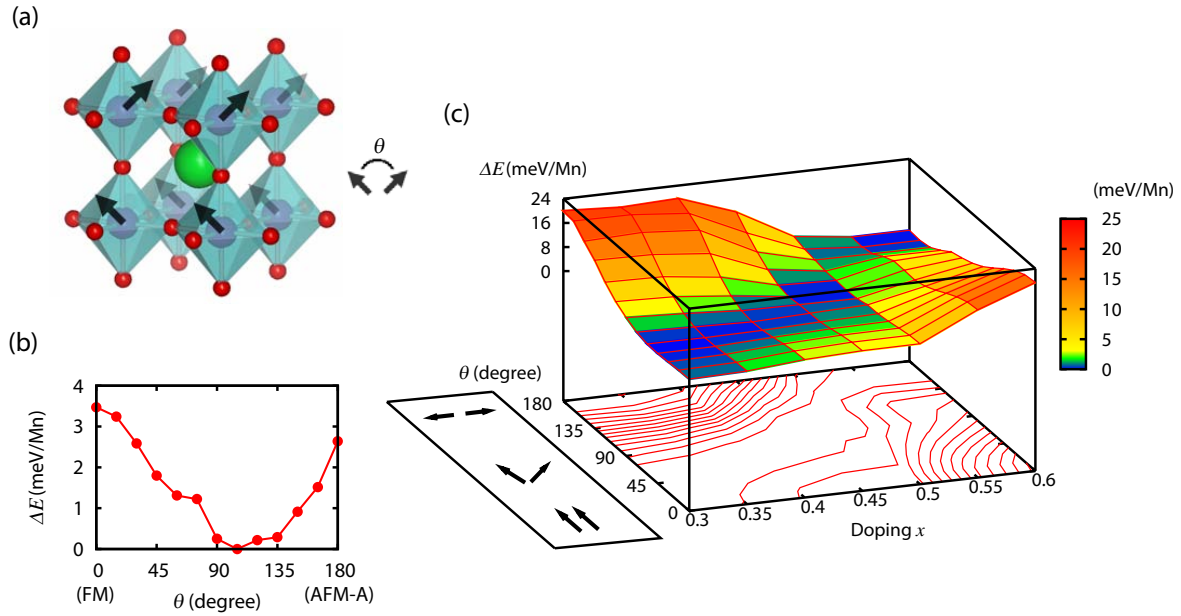
(a)

(c)

(b)

Figure 2. (a) The spin-canting magnetic structure of $La_{1-x}Sr_xMnO_3$ (LSMO). θ is the spin-canting angle between the interplane Mn sites. (b) The total energy difference per Mn atom from the stable state as a function of θ in LSMO ($x = 0.5$). (c) The total energy difference per Mn atom from the stable state in the parameter space as a function of hole doping x ($0.3 \leq x \leq 0.6$) and θ (degree). The change from blue to red in the color bar on the right-hand side represents the increase in the total energy difference. The lines serve as a visual reference.

3. Results

3.1. Stability of Collinear Magnetic States in $La_{1-x}Sr_xMnO_3$

We study the stability of the collinear magnetic states in LSMO. The calculated collinear magnetic states are the FM, AFM-A, AFM-C and AFM-G states (Fig. 1 (a)). Figure 1 (b) shows the total energy difference per Mn atom from the stable state as a function of x. In the case of $x = 0.0$ and $0.5 \leq x < 0.8$, the AFM-A state becomes stable. The FM state becomes stable in the region of $0.1 \leq x < 0.5$. The AFM-C state becomes stable around $x = 0.8$. The AFM-G state becomes stable in the region of $0.8 < x \leq 1.0$. The AFM order becomes favorable with increasing x in the region of $0.5 \leq x \leq 1.0$. This result is consistent with the previous theoretical and experimental studies[4, 5].

3.2. Noncollinear Magnetism in $La_{1-x}Sr_xMnO_3$

We extended the calculation of magnetic states for noncollinear configurations, as shown in Fig. 2 (a). In Fig. 1, $x = 0.5$ is the carrier concentration at which the total energies of the FM and AFM-A states are nearly degenerate within 1.0 meV/Mn. Figure 2 (b) indicates the total energy difference per Mn atom from the stable state as a function of θ. θ is defined as the interplane spin-canting angle, i.e., $\theta = 0°$ and $\theta = 180°$ correspond

to the FM and AFM-A states, respectively. We found that the SCM state ($\theta = 105°$) is stable for $x = 0.5$.

We also investigated the carrier dependence of the noncollinearity in the SCM state of LSMO ($0.3 \leq x \leq 0.6$). Figure 2 (c) shows the magnetic phase stability as a function of x and θ. ΔE denotes the total energy difference per Mn atom from the stable state. The SCM state is stable in the region of $0.3 \leq x \leq 0.6$. With increasing x, stable θ continuously increases from the FM ($\theta = 0°$) state and AFM-A ($\theta = 180°$) state.

4. Discussion

We discuss the stability of noncollinear magnetism around the magnetic phase boundary. It is understood that the carrier-induced magnetism in perovskite manganites is governed by the double exchange (DE) interaction[6, 32, 33]. The SCM state has been explained by the DE mechanism by de Gennes[6]. According to his theory, in addition to the AFM superexchange (SE) interaction, the FM interaction is caused by electron hopping from a half-filled e_g state to an empty e_g state with Hund's coupling. Then, the SCM states are stable because of the competition between the FM DE and AFM SE interactions in LSMO. Although de Gennes restricted his discussions to low carrier concentrations, Solovyev and Terakura extended de Gennes's theory to a wide region of carrier concentrations[7] and predicted that the SCM state may be stable around the half-doped concentration ($x = 0.5$). Our first-principles results are consistent with this prediction, and the SCM state is stable in the region of $0.3 \leq x \leq 0.6$. We suggest that a noncollinear magnetic state may appear in a wide range of hole-doped perovskite manganites.

We discuss the effect of lattice distortions in $x = 0.5$. We have performed a calculation of the cubic LSMO with an averaged lattice constant. The total energy difference between the FM and AFM-A states is 9.8 meV/Mn in $x = 0.5$. The corresponding energy difference in the orthorhombic structure is 0.8 meV/Mn. We predict that the SCM state is more stable in the orthorhombic structure than in the cubic structure. We also discuss why the total energy difference is large in the cubic structure. We attribute this difference to a decrease in the AFM SE interaction at the interplane. The average lattice constant in the cubic structure (3.873 Å) is larger than that in the orthorhombic structure (3.826 Å). The larger lattice constant leads to a decrease in the overlap between the wavefunctions of the interplane Mn atoms, i.e., the AFM SE interaction decreases at the interplane. Therefore, the lattice distortion may affect the stability of the noncollinear magnetic phase. We propose that the control of the noncollinear magnetic states is possible by the superlattice composition.

5. Summary

In summary, we have performed a noncollinear first-principles density-functional calculation on carrier-doped perovskite manganites LSMO. The calculated collinear

magnetic ground state was consistent with that reported in previous theoretical and experimental studies[4, 5]. Our calculations revealed that the noncollinear magnetic state is stable in LSMO ($0.3 \leq x \leq 0.6$). We discussed the stability of noncollinear magnetism in the magnetic phase boundary. Lattice distortions may change the stability of the noncollinear magnetic phase.

Acknowledgments

References

[1] Tokura Y, Urushibara A, Moritomo Y, Arima T, Asamitsu A, Kido G and Furukawa N 1994 *J. Phys. Soc. Japan* **63** 3931

[2] Okimoto Y, Katsufuji T, Ishikawa T, Urushibara A, Arima T and Tokura Y 1995 *Phys. Rev. Lett.* **75** 109

[3] Konishi Y, Fang Z, Izumi M, Manako T, Kasai M, Kuwahara H, Kawasaki M, Terakura K and Tokura Y 1999 *J. Phys. Soc. Japan* **68** 3790

[4] Fang Z, Solovyev I V and Terakura K 2000 *Phys. Rev. Lett.* **84** 3169

[5] Chmaissem O, Dabrowski B, Kolesnik S, Mais J, Jorgensen J D and Short S 2003 *Phys. Rev. B* **67** 094431

[6] de Gennes P G 1960 *Phys. Rev.* **118** 141

[7] Solovyev I V and Terakura K 2001 *Phys. Rev. B* **63** 174425

[8] Yoshizawa H, Kawano H, Tomioka Y and Tokura Y 1995 *Phys. Rev. B* **52** 13145

[9] Moreo A, Yunoki S and Dagotto E 1999 *Science* **283** 2034

[10] Nagaev E L 1998 *Phys. Rev. B* **58** 2415

[11] Yunoki S, Hu J, Malvezzi A L, Moreo A, Furukawa N and Dagotto E 1998 *Phys. Rev. Lett.* **80** 845

[12] Koida T, Lippmaa M, Fukumura T, Itaka K, Matsumoto Y, Kawasaki M and Koinuma H 2002 *Phys. Rev. B* **66** 144418

[13] Yamada H, Kawasaki M, Lottermoser T, Arima T and Tokura Y 2006 *Appl. Phys. Lett.* **89** 052506

[14] Izumi M, Murakami Y, Konishi Y, Manako T, Kawasaki M and Tokura Y 1999 *Phys. Rev. B* **60** 1211

[15] von Barth U and Hedin L 1972 *J. Phys. C: Solid State Phys.* **5** 1629

[16] Kübler J, Höck K H, Sticht J and Williams A R 1988 *J. Phys. F: Met. Phys.* **18** 469

[17] Perdew J P, Burke K and Ernzerhof M 1996 *Phys. Rev. Lett.* **77** 3865

[18] Troullier N and Martins J L 1991 *Phys. Rev. B* **43** 1993

[19] Louie S G, Froyen S and Cohen M L 1982 *Phys. Rev. B* **26** 1738

[20] Ozaki T 2003 *Phys. Rev. B* **67** 155108

[21] Ozaki T and Kino H 2004 *Phys. Rev. B* **69** 195113

[22] Kurz Ph, Förster F, Nordström L, Bihlmayer G and Blügel S. 2004 *Phys. Rev. B* **69**, 024415

[23] Gebauer R and Baroni S 2000 *Phys. Rev. B* **61** R6459

[24] Ozaki T, Kino H, Yu J, Han M J, Kobayashi N, Ohfuti M, Ishii F, Ohwaki T, Weng H and Terakura K, Available from: http://www.openmx-square.org/

[25] Picozzi S, Yamauchi K, Bihlmayer G and Blügel S 2006 *Phys. Rev. B* **74** 094402

[26] Han M J, Ozaki T and Yu J 2004 *Phys. Rev. B* **70** 184421

[27] Longo R C, Alemany M M G, Ferrer J, Vega A and Gallego L J 2008 *J. Chem. Phys.* **128** 114315

[28] Han M J, Ozaki T and Yu J 2006 *Phys. Rev. B* **73** 045110

[29] Han M J, Ozaki T and Yu J 2007 *Phys. Rev. B* **75** 060404(R)

[30] Alonso J A, Martinez-Lope M J, Casais M T and Fernandez-Diaz M T 2000 *Inorg. Chem.* **39** 917

[31] Negas T and Roth R S 1970 *J. Solid State Chem.* **1** 409

[32] Zener C 1951 *Phys. Rev.* **82** 403

[33] Anderson P W and Hasegawa H 1955 *Phys. Rev.* **100** 675